DECOMPOSITION AND ORDERING PROCESSES INVOLVING THERMODYNAMICALLY FIRST-ORDER ORDER → DISORDER TRANSFORMATIONS

W. A. SOFFA[1] and D. E. LAUGHLIN[2]

[1]Department of Materials Science and Engineering, University of Pittsburgh, PA 15260 and
[2]Department of Metallurgical Engineering and Materials Science, Carnegie-Mellon University,
Pittsburgh, PA 15213, U.S.A.

Abstract—Clustering and ordering processes often occur concomitantly or synergistically during the decomposition of supersaturated solid solutions. However, the occurrence of spinodal decomposition in conjunction with an order → disorder transformation thermodynamically of first order under equilibrium conditions is generally not well understood. In this paper a simple graphical approach using free energy-composition diagrams and loci of thermodynamic instability delineating regions of continuous transformation is used to develop a framework for understanding the interplay between clustering and ordering occurring in metallic solid solutions where the ordered precipitate stems from a phase diagram configuration in which the ordered and disordered states are connected by a first-order phase transition. The approach is applied to the Ni–Al, Ni–Ti and Al–Li binary alloy systems in which the interaction of clustering and ordering appears to play an important role.

Résumé—Les mécanismes de formation d'amas et de mise en ordre ont souvent lieu de façon concomitante ou synergique pendant la décomposition de solutions solides sursaturées. Cependant, on ne comprend généralement pas bien que la décomposition spinodale ait lieu en même temps qu'une transformation ordre → désordre thermodynamiquement du premier ordre dans des conditions d'équilibre. Dans cet article, nous utilisons une approche graphique simple qui utilise les diagrammes énergie libre-composition et les lieux d'instabilité thermodynamique limitant les régions de transformation continue; cette approche nous permet de développer une structure pour comprendre le rôle joué par la formation d'amas et par la mise en ordre dans des solutions solides métalliques où le précipité ordonné naît d'une configuration du diagramme de phases dans lequel les états ordonné et désordonné sont reliés par une transition de phases du premier ordre. Cette approche est appliquée aux systèmes des alliages binaires Ni–Ti et Al–Li pour lesquels l'interaction de la formation d'amas et de la mise en ordre semble jouer un rôle important.

Zusammenfassung—Prozesse des Clusterns und der Ordnungseinstellung treten häufig zusammen oder synergistisch während der Entmischung übersättigter Mischkristalle auf. Das Auftreten der spinodalen Entmischung zusammen mit einer Umwandlung Ordnung → Entordnung, thermodynamisch von erster Ordnung, unter Gleichgewichtsbedingungen ist allerdings im allgemeinen nicht gut verstanden. In dieser Arbeit wird ein einfaches grafisches Verfahren benutzt, um einen Rahmen für das Verständnis des Wechselspieles zwischen Clustern und Ordnungseinstellung in metallischen Mischkristallsystemen zu entwickeln. Das Verfahren benutzt Diagramme der freien Energie über der Zusammensetzung und Orte der thermodynamischen Instabilität, welche Bereiche der kontinuierlichen Umwandlung abgrenzen. In den Mischkristallen stammen die geordneten Ausscheidungen aus einer Konfiguration des Phasendiagrammes, in der die geordneten und entordneten Zustände über eine Phasenumwandlung erster Ordnung miteinander verbunden sind. Das Verfahren wird auf die binären Legierungssysteme Ni–Al, Ni–Ti und Al–Li angewendet, in denen die Wechselwirkung der Clusterbildung und Ordnungseinstellung eine wichtige Rolle zu spielen scheinen.

1. INTRODUCTION

1.1. General

It is well-established both experimentally and theoretically that clustering and ordering are not mutually exclusive processes in undercooled or supersaturated metallic solid solutions, but often proceed concomitantly or synergistically during the decomposition of a quenched alloy [1–5]. This has been particularly elucidated in systems such as Fe–Al binary alloys where the order → disorder transformation (A2 → B2)

is second, or higher, order [1]. However, the occurrence of spinodal decomposition in conjunction with a metastable or stable order → disorder transformation thermodynamically of first-order under equilibrium conditions, e.g. Al → L1$_2$ is generally not well understood. There does exist a plethora of data suggesting that spinodal decomposition and ordering occur together to produce the characteristic resultant microstructures consisting of a disordered (α) phase and an ordered (γ) phase, e.g. Ni–Al [6, 7] and Ni–Ti [8, 9]. However, the systematics of mapping the
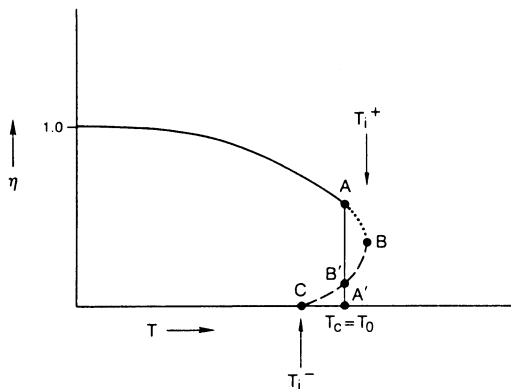
Fig. 1. Characteristic variation of the long range order parameter (η) with temperature for an order/disorder transformation thermodynamically of first order.

regions of instability with respect to clustering and/or ordering (disordering) in a thermodynamically self-consistent manner with respect to the phase diagram and has not been comprehensively addressed.

In this paper a simple approach using free energy–composition diagrams and *loci* of thermodynamic instability delineating regions of continuous phase transformation is used to suggest a framework for understanding the often complex interplay between clustering and ordering occurring in metallic solid solutions where the ordered phase which emerges from the initially disordered solid solution stems from a phase diagram configuration in which the disordered and ordered states are connected by a first-order transition under equilibrium conditions. The essentially graphical thermodynamic method embodies the concepts and results of various more quantitative analytical approaches but is not constrained by the usual limitations of particular solution models. The treatments by Kulkarni *et al.* [10] and Khachaturyan *et al.* [11] in particular, have
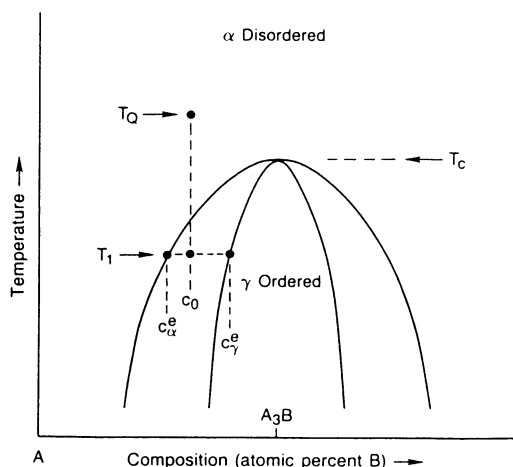
identified some important aspects of the problem which will be extended and expounded upon herein. The influence of elastic energy on phase stability and equilibria are not taken into account in the analysis which follows.

1.2. Review of some basic concepts relating to first-order order → disorder transformations

Figure 1 shows the characteristic variation of the long range order (LRO) parameter with temperature for the stoichiometric A_3B composition indicated in the phase diagram shown in Fig. 2. The order parameter which describes the atomic arrangement is proportional to the amplitude of the concentration wave associated with the particular superstructure [12, 13]. At the temperature $T = T_c$, the ordered state A ($\eta \neq 0$) is in thermodynamic equilibrium with the disordered state A' ($\eta = 0$). This equilibrium is depicted in the familiar Landau plot of the free energy vs order parameter in Fig. 3(a). Also shown in Fig. 3(a) are free energy curves for temperatures above $T = T_c$. Along the dotted durve in Fig. 1 from A to B there exists a metastable ordered state $\eta = \eta' \neq 0$, and the disordering of the superheated ordered phase must occur by a heterogeneous process involving nucleation and growth of the disordered phase within the metastable ordered phase. At the point B, $T = T_i^+$, the superheated ordered phase is unstable with respect to disordering and this con-

Fig. 2. Typical phase diagram configuration associated with a first order transformation
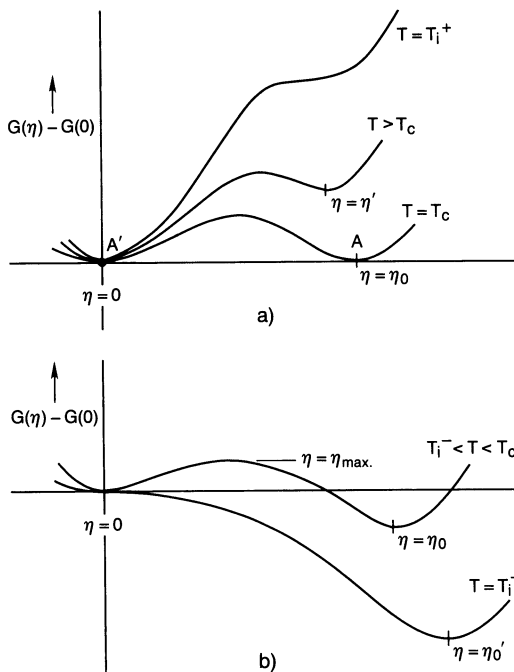

a)

b)

Fig. 3. Free energy curves showing the variation of $G(\eta) - G(0)$ with temperature and order parameter. $G(\eta)$ is the free energy of the ordered phase in the ordered state η and $G(0)$ is the free energy of the disordered state.
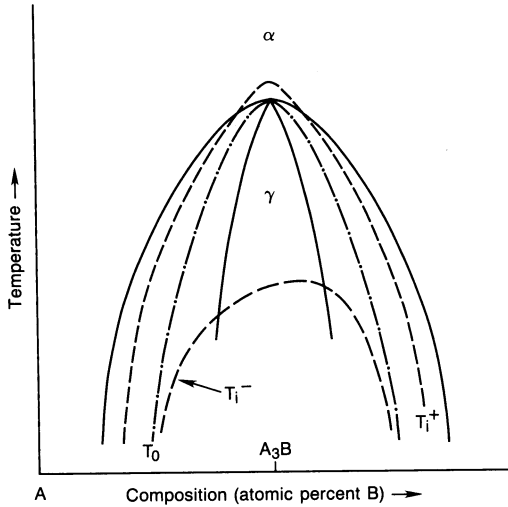
Fig. 4. Schematic order/disorder phase diagram with superposed instability *loci* T_i^- and T_i^+. Also shown in the diagram is the temperature T_0 where the free energies of the ordered phase and disordered phase are equal.

dition is depicted in Fig. 3(a). Thus, T_i^+ is a disordering instability temperature and for $T \geqslant T_i^+$ a superheated ordered solid solution will disorder homogeneously or continuously. Similarly, on cooling a disordered solid solution below T_c, for temperatures $T_i^- < T < T_c$, the free energy vs order parameter curves exhibit a thermodynamic barrier between the undercooled disordered state ($\eta = 0$) and the ordered state $\eta = \eta_o \neq 0$, as shown in Fig. 3(b). The locus from B' to C in Fig. 1 is the value of η at the maximum point (η_{max}). In the temperature regime $T_i^- < T < T_c$ an undercooled disordered phase can only order heterogeneously by nucleation and growth. At the temperature T_i^-, the ordering instability, the barrier vanishes and the free energy is monotonically decreasing from $\eta = 0$ to $\eta = \eta_0'$, the equilibrium ordered state. The disordered state is unstable with respect to ordering and an undercooled disordered state will be able to order homogeneously or continuously (spinodal ordering) involving the spontaneous amplification of the specific concentration or ordering wave throughout the system without the need for a nucleation step.

This discussion can be generalized and extended to off-stoichiometric compositions [11]. The ordering (T_i^-) and disordering (T_i^+) instabilities are superposed on the phase diagram in Fig. 4 as well as the locus T_0 delineating the point where the ordered and disordered phases have identical free energies at a given composition. The ordering instability locus can be estimated at low temperatures using the method of concentration waves by Khachaturyan [12, 13] and is given by

$$T_i^- = \frac{-2V(\bar{k})c(1-c)}{k_B} \qquad (1)$$

where $V(\bar{k})$ for the wave vector $\bar{k}$ of the concentration

wave is related to the Fourier transform of the pair interaction parameter V_i, defined by

$$V_i = E_{AB}^i - \tfrac{1}{2}(E_{AA}^i + E_{BB}^i) \qquad (2)$$

where E_{AB}^i, E_{AA}^i and E_{BB}^i are the AB, AA and BB pairwise interaction or bond energies in the ith nearest-neighbor shell, respectively. Ordering instabilities are associated with "special points" in $\bar{k}$-space where the function $V(\bar{k})$ is an extremum. Clustering instabilities are associated with the term $V(0)$ in this formalism [14].

2. APPROACH TO CLUSTERING AND ORDERING: GRAPHICAL THERMODYNAMICS

The free energy-composition scheme shown in Fig. 5 is consistent with the simple order → disorder phase diagram in Fig. 2 at temperature T_1. The common tangent construction establishes the equilibrium between the disordered (α) and ordered (γ) conjugate phases of compositions C_α^e and C_γ^e, respectively, at the temperature T_1 for a solution of overall composition C_0. If a solid solution of composition C_0 is rapidly quenched from T_Q in the single phase field to T_1 essentially retaining the disordered state, the disordered solution α_0 would have a free energy given by point A in Fig. 5. The system can reduce its free energy to B by decomposing into a two-phase mixture ($\alpha_E + \gamma_E$), the relative proportions of the conjugate phases given by the lever rule. (This neglects the possible effects of coherency strains. See, e.g. [15–17].) The initial state A (supersaturated solution α_0) is metastable with respect to precipitation of the ordered γ phase because the curvature of the free energy-composition curve for the disordered α_0 phase is positive or concave upward. The reaction path taking the system from A to B must involve the *nucleation and growth* of the *ordered* phase within the disordered phase to produce the equilibrium mixture.
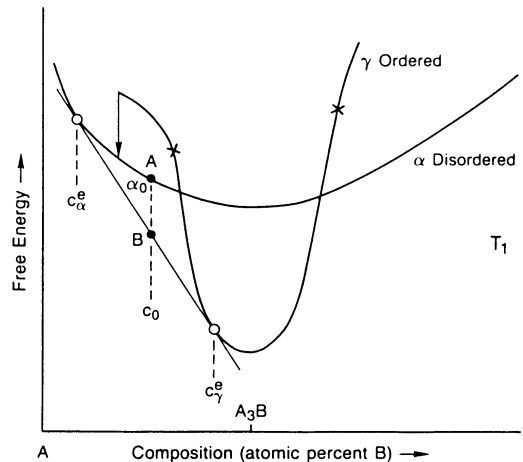

Fig. 5. Schematic free energy vs composition diagram for the ordered and disordered phases at T_1. The arrow denotes the limit of stability of the ordered phase.
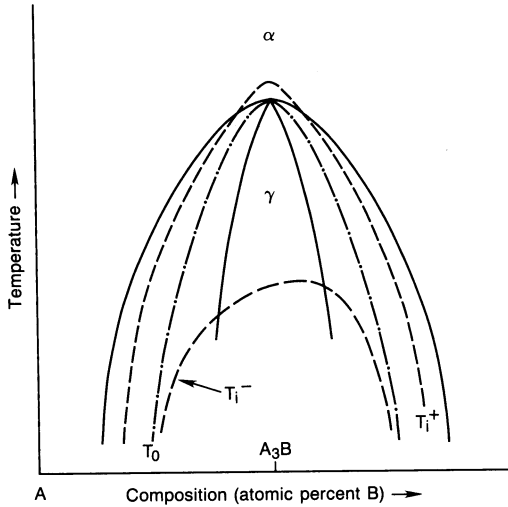
Fig. 4. Schematic order/disorder phase diagram with super-posed instability *loci* T_i^- and T_i^+. Also shown in the diagram is the temperature T_0 where the free energies of the ordered phase and disordered phase are equal.

dition is depicted in Fig. 3(a). Thus, T_i^+ is a dis-ordering instability temperature and for $T \geqslant T_i^+$ a superheated ordered solid solution will disorder homogeneously or continuously. Similarly, on cool-ing a disordered solid solution below T_c, for tem-peratures $T_i^- < T < T_c$, the free energy vs order parameter curves exhibit a thermodynamic barrier between the undercooled disordered state ($\eta = 0$) and the ordered state $\eta = \eta_o \neq 0$, as shown in Fig. 3(b). The locus from B′ to C in Fig. 1 is the value of η at the maximum point (η_{max}). In the temperature regime $T_i^- < T < T_c$ an undercooled disordered phase can only order heterogeneously by nucleation and growth. At the temperature T_i^-, the ordering instabil-ity, the barrier vanishes and the free energy is monotonically decreasing from $\eta = 0$ to $\eta = \eta_0'$, the equilibrium ordered state. The disordered state is unstable with respect to ordering and an undercooled disordered state will be able to order homogeneously or continuously (spinodal ordering) involving the spontaneous amplification of the specific concen-tration or ordering wave throughout the system without the need for a nucleation step.

This discussion can be generalized and extended to off-stoichiometric compositions [11]. The ordering (T_i^-) and disordering (T_i^+) instabilities are super-posed on the phase diagram in Fig. 4 as well as the locus T_0 delineating the point where the ordered and disordered phases have identical free energies at a given composition. The ordering instability locus can be estimated at low temperatures using the method of concentration waves by Khachaturyan [12, 13] and is given by

$$T_i^- = \frac{-2V(\bar{k})c(1-c)}{k_B} \qquad (1)$$

where $V(\bar{k})$ for the wave vector $\bar{k}$ of the concentration

wave is related to the Fourier transform of the pair interaction parameter V_i, defined by

$$V_i = E_{AB}^i - \tfrac{1}{2}(E_{AA}^i + E_{BB}^i) \qquad (2)$$

where E_{AB}^i, E_{AA}^i and E_{BB}^i are the AB, AA and BB pairwise interaction or bond energies in the ith nearest-neighbor shell, respectively. Ordering in-stabilities are associated with "special points" in $\bar{k}$-space where the function $V(\bar{k})$ is an extremum. Clustering instabilities are associated with the term $V(0)$ in this formalism [14].

2. APPROACH TO CLUSTERING AND ORDERING: GRAPHICAL THERMODYNAMICS

The free energy-composition scheme shown in Fig. 5 is consistent with the simple order → disorder phase diagram in Fig. 2 at temperature T_1. The common tangent construction establishes the equi-librium between the disordered (α) and ordered (γ) conjugate phases of compositions C_α^e and C_γ^e, respect-ively, at the temperature T_1 for a solution of overall composition C_0. If a solid solution of composition C_0 is rapidly quenched from T_Q in the single phase field to T_1 essentially retaining the disordered state, the disordered solution α_0 would have a free energy given by point A in Fig. 5. The system can reduce its free energy to B by decomposing into a two-phase mixture ($\alpha_E + \gamma_E$), the relative proportions of the conjugate phases given by the lever rule. (This neglects the possible effects of coherency strains. See, e.g. [15–17].) The initial state A (supersaturated solution α_0) is metastable with respect to precipitation of the ordered γ phase because the curvature of the free energy-composition curve for the disordered α_0 phase is positive or concave upward. The reaction path taking the system from A to B must involve the *nucleation and growth* of the *ordered* phase within the disordered phase to produce the equilibrium mixture.
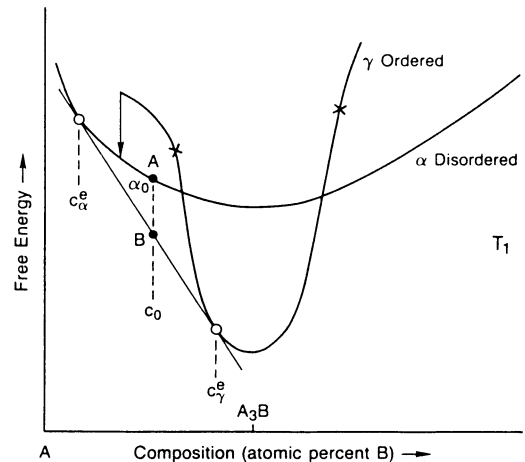

Fig. 5. Schematic free energy vs composition diagram for the ordered and disordered phases at T_1. The arrow denotes the limit of stability of the ordered phase.
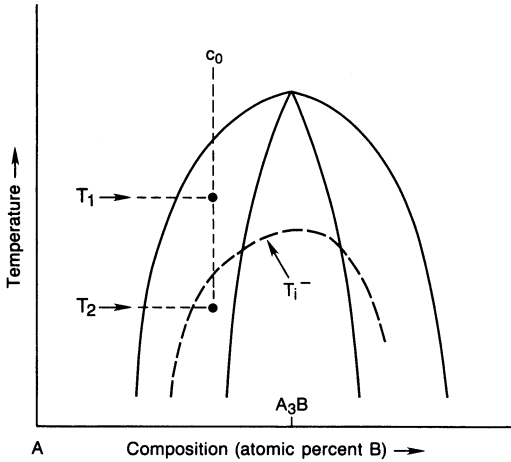
Fig. 6. Schematic phase diagram showing the ordering instability T_i^-. The solution of composition C_0 is metastable at T_1 but unstable at T_2 with respect to ordering.

Fig. 8. Schematic free curves in $G–c–\eta$ space. Points P, P′ and R represent different states of thermodynamic stability of the disordered phase with respect to ordering.

If the α solid solution is quenched to T_2 below the ordering instability T_i^- as depicted in Fig. 6, a continuous transformation path becomes accessible to the system. The free energy-composition diagram for $T = T_2$ is given in Fig. 7. The hatched portion of the free energy curve of the disordered α phase represents solution compositions which are unstable with respect to ordering, and these initial or as-quenched states will continuously order relaxing the free energy progressively from point A′ to B′. The homogeneously ordered, single-phase state B′ is metastable with respect to the formation of the stable two-phase mixture and the free energy of the system can be reduced further to C′ only by *nucleation* of the *disordered* phase.

The thermodynamic stability of the quenched state A′ in Fig. 7 can be illustrated by recalling that

stability with respect to ordering derives from the variation of the free energy with respect to the order parameter η as depicted in Fig. 8. The state P in this diagram is unstable with respect to ordering since the free energy is monotonically decreasing to the ordered state characterized by $\eta_0^* > 0$. The initial disordered solid solution ($\eta = 0$) at point P will *continuously order* to η_0 at point Q to produce a homogeneous, ordered single-phase state of lower free energy without a nucleation step. An as-quenched α solid solution at P′ outside the hatched region, however, is metastable with respect to ordering since there is a free energy barrier between the initial disordered state ($\eta = 0$) and the more stable ordered state at Q′. Thus, a *congruent ordering* process as defined by Khachaturyan *et al.* [11], taking the system from P′ to Q′ without a composition change,
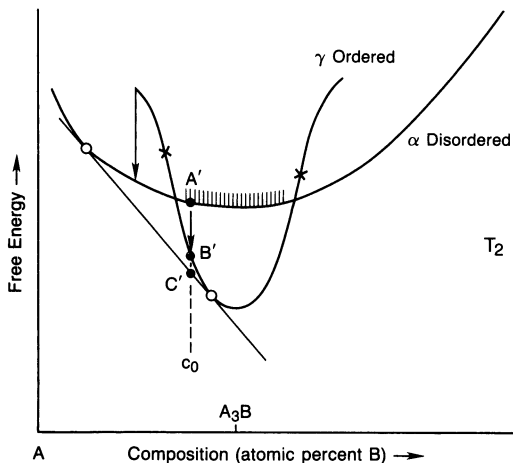

Fig. 7. Schematic free energy vs composition diagram for the ordered and disordered phases at T_2. The hatched segment of the free energy curve for the disordered phase corresponds to solutions which are unstable with respect to continuous ordering.
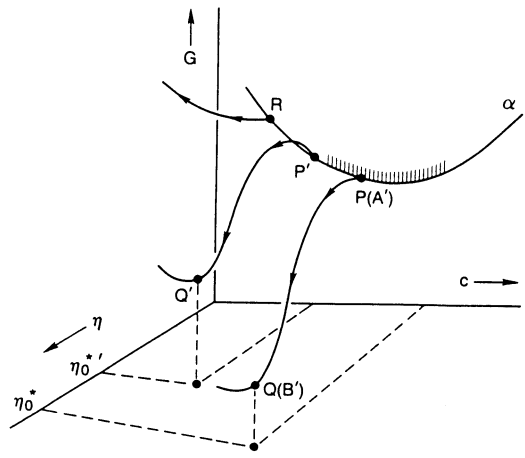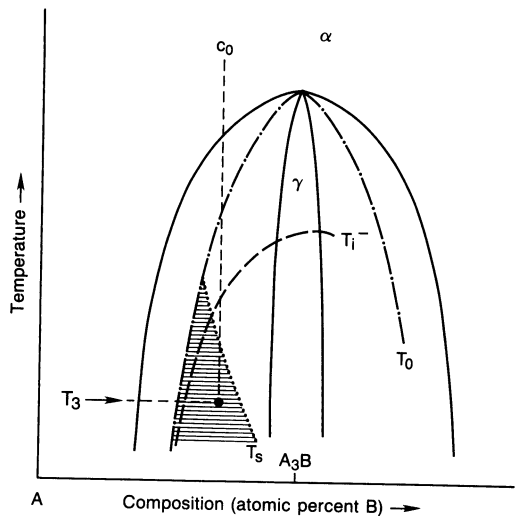

Fig. 9. Phase diagram including a spinodal region (with respect to phase separation) in addition to the region of ordering instability below T_i^-.
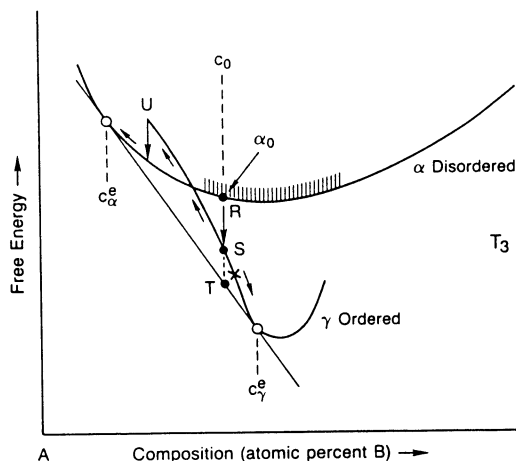
Fig. 10. Schematic free energy vs composition diagram for the ordered and disordered phases at T_3. Note the appearance of a spinodal ($G'' = 0$) in the ordered phase and a region of thermodynamic instability with respect to phase separation contingent on prior atomic ordering

can only occur by nucleation and growth of ordered regions within the disordered α phase. The as-quenched solution corresponding to point R on the free energy curve for the disordered α phase in Fig. 8 is stable with respect to ordering. Clearly, this point lies to the left of the intersection of the free energy curves or to the left of T_0 in Fig. 4 which delineates the locus where the free energies of the single-phase ordered and disordered solutions are equal.

If a solution of composition C_0 is quenched to T_3 as in Fig. 9, the relevant free energy-composition diagram is shown schematically in Fig. 10. The initial disordered α_0 solid solution is unstable with respect to ordering and will continuously order to the homogeneous ordered, single-phase state with free energy given by point S. The ordered solution is

thermodynamically unstable with respect to phase separation since at S the curvature of the free energy-composition curve is negative. *Spinodal decomposition* will occur initially into two ordered phases of different compositions and as the spinodal process proceeds the compositions of the emerging phases will move along the free energy curve as shown by the arrows in Fig. 10. At point U the ordered phase, depleted in solute, disorders spontaneously (continuous disordering) and equilibrium between the disordered (C_α^e) and ordered (C_γ^e) phases is established.

The different regimes of transformation are shown more clearly in Fig. 11. The shaded regions (hatched and cross-hatched) delineate the temperatures and solution compositions for which an ordered single-phase state is unstable with respect to phase separation. The left-hand boundary is the locus T_0 and the right-hand boundary is the spinodal composition for the ordered (γ) free energy curve. In the shaded region between T_0 and T_i^- (cross-hatched), the as-quenched state α_0 is *metastable with respect to ordering*; thus, the single phase ordered state which spinodally decomposes can only be reached by a *congruent ordering* reaction prior to phase separation. In the hatched region between T_i^-, the ordering instability, and the spinodal curve, T_s, the as-quenched, disordered solutions α_0 are unstable with respect to continuous ordering and subsequently the ordered states are unstable with respect to phase separation. This situation is the *conditional spinodal* where spinodal decomposition is contingent on prior ordering [1].

From this graphical thermodynamic description based simply on the topological properties of the free energy curves or surfaces (the argument is actually carried out in G–c–η space) of the ordered and disordered phases, it is easy to predict various non-equilibrium reaction paths giving rise to the equilibrium two-phase mixture involving an interplay between clustering and ordering. As discussed by various authors [4, 18] such phenomena require pairwise interactions involving at least second-nearest neighbors. Importantly, in the case of the thermodynamically first-order order → disorder transformation discussed above, a *spinodal decomposition* process resulting in a two-phase mixture of ordered and disordered phases at equilibrium *always involves prior ordering* of the solution, either by congruent (heterogeneous) or continuous (homogeneous) ordering. Furthermore, the thermodynamic analysis identifies a possible transformation mode—the congruent ordering process—whereby a disordered, single-phase state transforms to an ordered, single-phase state without composition change via nucleation and growth of ordered regions within the metastable disordered solution. This compositionally invariant phase change is not well-documented in the literature but has been discussed by Khachaturyan *et al.* [11]. The characteristics of such a heterogeneous ordering are clearly akin to a massive transformation [19, 20].
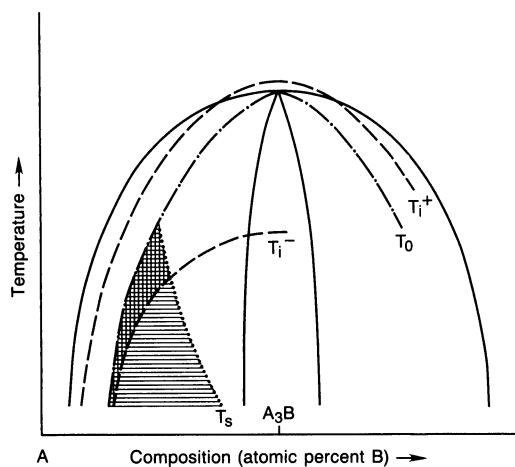

Fig. 11. Phase diagram showing the different regimes of thermodynamic stability with respect to disordering (T_i^+), ordering (T_i^-) and phase separation (T_s). Also delineated is the region of possible congruent ordering.
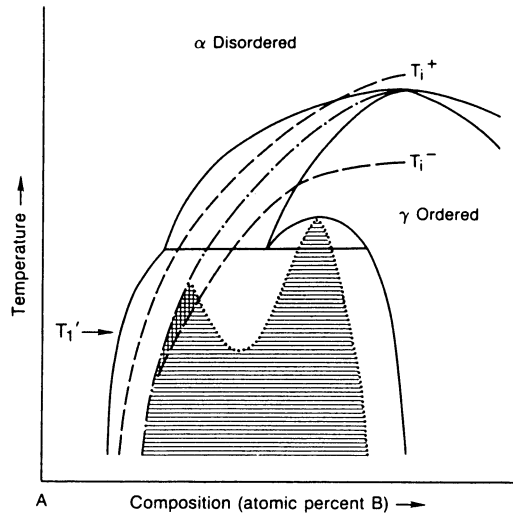
Fig. 12. Phase diagram configuration showing a monotectoid reaction involving the ordered and disordered phases, including the various regimes of thermodynamic instability.

Fig. 14. Metastable miscibility gap associated with the homogeneously ordered phase.

Complex solution energetics can produce other phase diagram configurations such as that shown in Fig. 12 exhibiting a monotectoid reaction isotherm. Again the shaded regions delineate single-phase ordered states which are unstable with respect to phase separation, and solutions quenched into these regions will order and then spinodally decompose. A free energy-composition curve for the temperature T_1' is shown in Fig. 13. Two regions of negative curvature appear in the free energy curve for the ordered phase; the second region actually produces a stable miscibility gap in the ordered, γ-phase field at higher temperatures. A possible variation of this behavior is the occurrence of a metastable miscibility gap in the homogeneously ordered phase as shown in Fig. 14. Notice that the metastable miscibility gap represent-
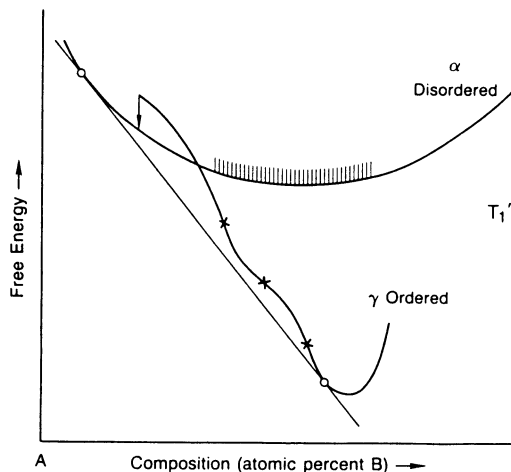
ing metastable equilibrium between two ordered phases terminates when the two spinodals merge.

An even more complex behavior can be envisioned involving a syntectoid reaction isotherm. Here the disordered solid solution can exhibit a miscibility gap at elevated temperatures merging with a first-order, ordering reaction at lower temperatures. A schematic phase diagram is shown in Fig. 15. A hypothetical free energy scheme is included in Fig. 16.

Various combinations of ordering and clustering, homogeneous and heterogeneous reaction, phase separation and precipitation can be predicted based on the simple principles illustrated above. For

Fig. 13. Free energy vs composition diagram at T_1' for the phase diagram shown in Fig. 12. Note the two regions of negative curvature appearing in the free energy curve of the ordered phase.
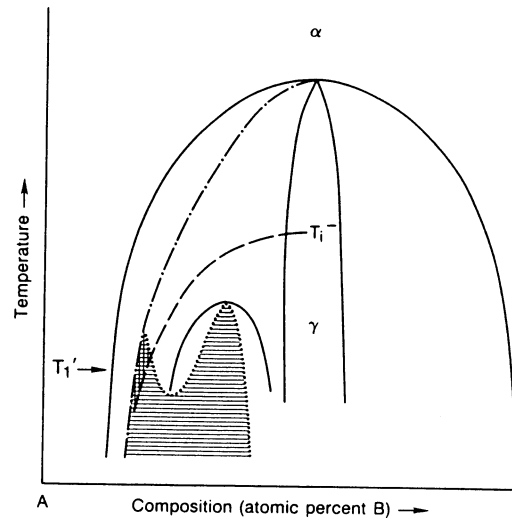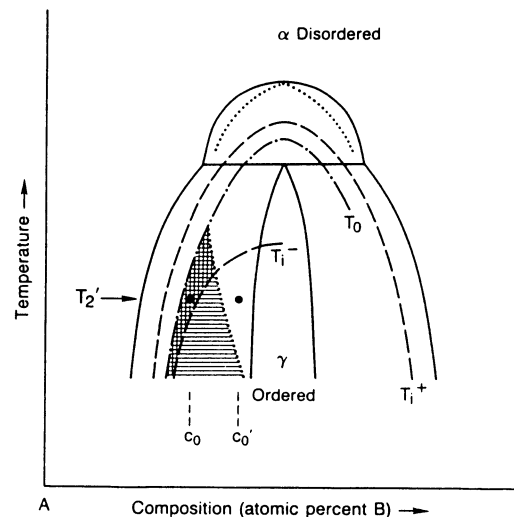

Fig. 15. Schematic phase diagram showing a miscibility gap in the disordered phase at higher temperatures and a first order order/disorder reaction at lower temperatures, combining to produce a *syntectoid* reaction isotherm. The various clustering and ordering instabilities have been included.
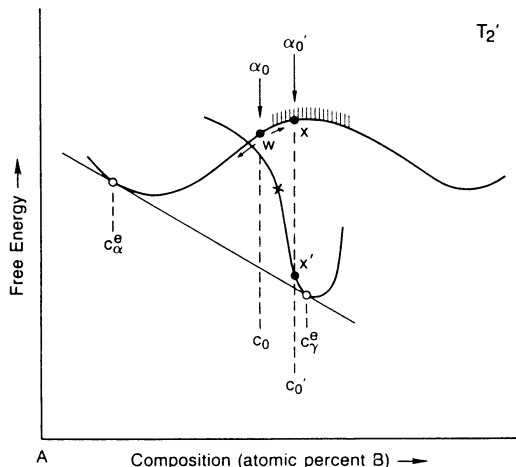
Fig. 16. Schematic free energy vs composition diagram corresponding to T_2' in Fig. 15. The different reaction paths followed by the disordered states α_0 and α_0' are determined by the thermodynamic stability of their initial state, W and X, respectively.

example, the as-quenched disordered solid solution α_0 of composition C_0 in Fig. 16 (point W) will initially spinodally decompose into two disordered phases. The solute-enriched regions will continuously order at some critical concentration to produce the ordered γ phase. The consecutive continuous transformations (phase separation and ordering) ultimately produce an equilibrium two-phase mixture of α (disordered) of composition, C_α^e, and γ (ordered) of composition, C_γ^e. A particularly interesting case is the supersaturated solution α_0' at X in Fig. 16. This as-quenched, dis-ordered solution at T_2' is initially unstable with respect to phase separation and ordering; however, the continuous ordering process involving only short-range atomic exchanges will occur faster and the free

energy will relax to X'. This renders the ordered solution metastable and the equilibrium two-phase mixture will evolve via nucleation and growth of the disordered phase.

3. DISCUSSION

The graphical thermodynamic approach developed above can be applied to three well-studied binary alloy systems, viz. Ni–Al, Ni–Ti and Al–Li in which the interaction of clustering and ordering appears to play a critical role in controlling the precipitation of a coherent, stable or metastable $L1_2$ phase within a nominally f.c.c. matrix. The equilibrium Al→$L1_2$ disorder→order transformation is first-order but at high supersaturations or undercoolings the occur-rence of a spinodal reaction in conjunction with the formation of the ordered phase has been suggested by numerous investigators.

3.1. Nickel–aluminum alloys

The equilibrium $Ni_3Al(\gamma')$ exhibits the $L1_2$ super-structure and is essentially the precipitating phase in numerous high-temperature, high-strength super-alloys. Supersaturated alloys containing more than about 10 at.% aluminum exhibit a "side-band state" during aging indicative of a modulated structure; however, Ardell and Nicholson with Eshelby [21] have shown that a non-random, aligned arrangement of particles can evolve from an initially random array through stress-affected diffusion during coarsening, and thus the modulated structure is clearly not a sufficient criterion for identifying a continuous phase separation process (spinodal decomposition). Atom probe field-ion microscopy (APFIM) analysis of a Ni–14 at.% Al alloy aged at 550°C reported by Wendt and Haasen [22] suggests that decomposition of the alloy follows a path of classical nucleation and growth. Hill and Ralph [23, 24] on the other hand have performed a combined TEM and APFIM study of a 14.1 at.% Al alloy aged at 625°C and based on analysis of the concentration profiles obtained with the "atom probe" have concluded that the formation of the Ni_3Al phase involves a continuous phase separation or spinodal decomposition process in con-junction with atomic ordering. The conclusions of Hill and Ralph are essentially in agreement with the transformation behavior described above and more clearly established in the Ni–Ti system described below. Gentry and Fine [6] and Corey et al. [7] in their earlier studies of the phase transformation mech-anism indicated that spinodal decomposition was involved in the formation of the ordered precipitate phase. However, it is concluded here that the de-composition path may be extremely sensitive to the actual quenching rate and that more work is required to elucidate the transformation mechanism. The new SANS studies by Kostorz and co-workers [25] in tandem with further APFIM and HREM
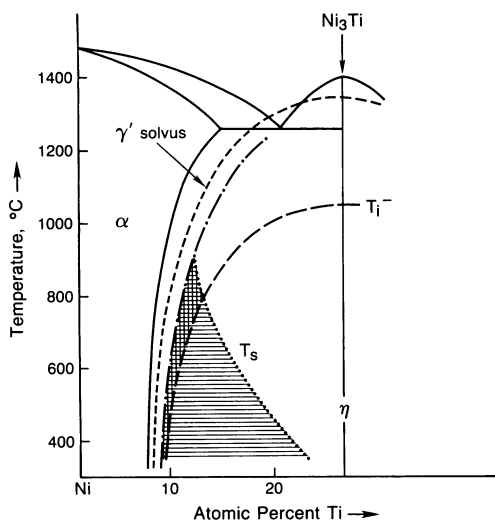

Fig. 17. Schematic phase diagram of the Ni-rich end of the Ni–Ti binary system, including *loci* of thermodynamic instability T_i^- and T_s.
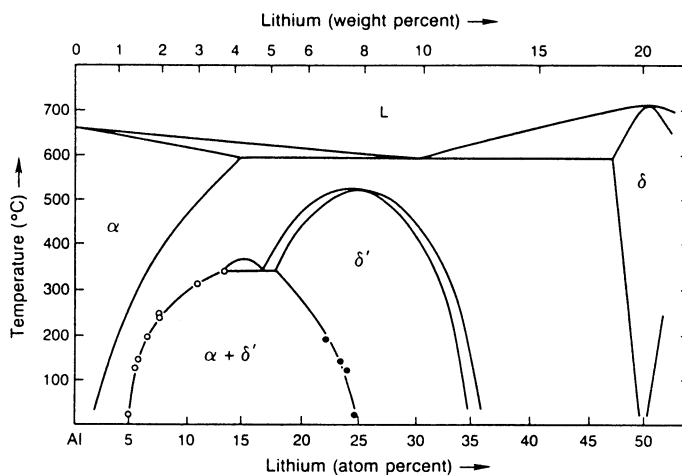
Fig. 18. Proposed phase diagram of the Al-rich end of the Al–Li binary system, including the metastable δ' phase, after Gayle and Vander Sande [30].

studies hold the best promise for clarifying the decomposition path in the Ni–Al alloys.

3.2. Ni–Ti alloys

The Ni–Ti binary system is generally of the same *genre* as the Ni–Al alloys and also of great importance in the metallurgy of superalloys since Ti along with Al is primary in the formation of the γ' phase. Figure 17 shows a schematic of the Ni-rich section of the Ni–Ti phase diagram. The equilibrium Ni_3Ti (η) phase is hexagonal but at high supersaturations a metastable γ' (Ni_3Ti; $L1_2$) phase precedes the formation of the stable η in alloys containing about 10 at.%

Fig. 19. Proposed phase diagram of the Al-rich end of the Al–Li binary system, including the metastable δ' phase, after Sigli and Sanchez [31]. Note that the miscibility gap suggested by these authors is with respect to the disordered supersaturated solid solution.

Ti or more. Various experimental approaches have been applied to elucidate the decomposition process involving clustering and ordering including magnetic measurements [26], electron microscopy and diffraction [3, 8], high-resolution electron microscopy (HREM) [27], small-angle neutron scattering (SANS) [28], and atom probe field-ion microscopy (APFIM) [9, 29]. A careful analysis of the data suggests that the formation of the metastable γ' phase generally occurs through a simultaneous composition modulation and atomic ordering, and that this *coupled continuous transformation* is preceded by continuous ordering of the matrix. This is consistent with the transformation *loci* shown in Fig. 17. Except for the window at low supersaturations, the decomposition of supersaturated alloys at low and moderate temperatures (500–700°C) will be characterized by continuous ordering ($L1_2$) followed by spinodal decomposition producing a metastable mixture of the α' terminal solid solution and γ' (Ni_3Ti; $L1_2$). This is essentially the mechanism suggested by Sinclair *et al.* [9] in their atom probe analysis of the precipitation reaction. This is also consistent with the recent results of Kostorz and co-workers [27, 28] using HREM and SANS. These high-resolution electron microscopy and neutron scattering experiments clearly indicate that the γ' phase evolves via the amplification of a concentration wave within an imperfectly *ordered* solid solution. Rapidly quenched specimens exhibit an $L1_2$ peak in electron (and X-ray) diffraction, and this is followed by the development of a broad SANS peak during the early stages of aging, which subsequently grows and sharpens with little change in position. The atom probe results of Grune and Haasen [29] show that for a Ni–12 at.% Ti alloy aged 256 h at 550°C, the composition *maxima* in the decomposing solid solution are still below the Ni_3Ti composition. It is concluded here that the Ni–Ti system is an excellent illustration of the continuous transformation behavior discussed in this paper; the
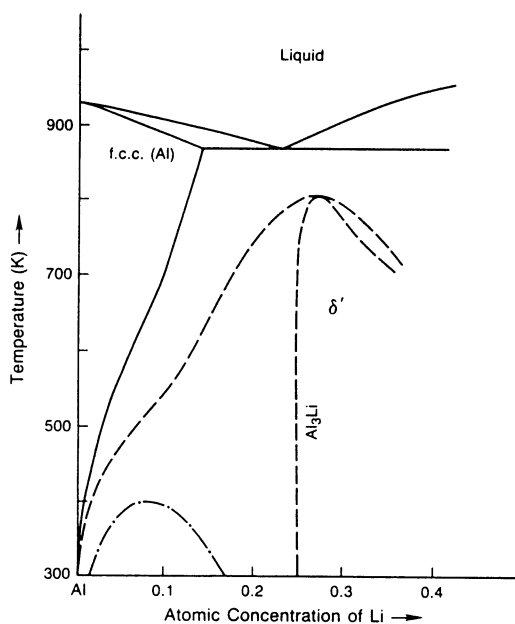
spinodal process occurring in the Ni–Ti alloys is generally contingent on prior ordering and the schematic transformation diagram mapped into the binary phase diagram properly describes the general synergistics of clustering and ordering in this type of binary system.

3.3. Al–Li alloys

The Al-rich end of the Al–Li phase diagram exhibits a metastable, two-phase region, between an α', f.c.c. terminal solid solution and the δ' phase, Al_3Li (Cu_3Au, $L1_2$). The latter phase forms from the supersaturated solution of Li in Al at low temperatures, and is responsible for the good mechanical properties of the alloys. Although the alloy system has been studied by many investigators, e.g. [30–34], the details of this two-phase equilibrium between the δ' phase and the Al-rich solid solution are not known.

To date, the main difficulty has been the fact that the thermodynamically *first order* order → disorder transition appears to be associated with a miscibility gap. Several attempts to identify this phase equilibrium have been made. Gayle and Vander Sande [30] have posited that a miscibility gap exists for the disordered phase and this gap joins the ordered phase region via a monotectoid configuration (see Fig. 18). Such a diagram accounts for both phase separation and atomic ordering. However, if it were to be modeled by pairwise interaction energies, the parameters would have to be strong functions of composition. Sigli and Sanchez [31] have proposed a metastable miscibility gap of the disordered phase within the two-phase region of the phase diagram (see Fig. 19). This diagram also could account for the observed clustering and ordering. However, there is as yet no explicit evidence that phase separation of a *disordered* phase exists in this alloy system. The basic findings of investigations to date are that the as-quenched alloys show evidence of ordering, and that at low temperatures, differential scanning calorimetry (DSC) shows that two peaks, related to the absorption of heat, occur during the heating of the specimens. This absorption of heat could be due to the dissolution of *either* a disordered or ordered phase; hence no conclusions can be made concerning the structure of the metastable low temperature phase by DSC.

Recently, Sato *et al.* [34] showed, in specimens of Al–9.7 at.% Li that are in the early stages of transformation, the alloys display ordered domains that are percolated throughout the microstructure. The ordered regions have an imperfect $L1_2$ structure, with boundaries that are very diffuse. The degree of order is lower in these regions than in the fully developed $L1_2$ phase.

All of the experimental findings on this system can be explained by the simple diagram essentially proposed by Khachaturyan *et al.* [11] and modified by Laughlin and Soffa [35] (see Fig. 11). Such a diagram

has the advantage of being quite simple, and can be modeled by pairwise interaction without any drastic changes in the interaction energies as a function of composition and/or temperature. Laughlin and Soffa [35] have also presented other diagrams that are consistent with the findings in systems such as Al–Li. Figure 14 shows a diagram with a *metastable* miscibility gap involving two ordered phases, and Figure 12 shows one where the ordered phase decomposes via a monotectoid reaction. While each of these diagrams are possible in the Al–Li system, further experimental work is required to establish which configuration obtains in the Al–Li system.

4. SUMMARY

A simple graphical thermodynamic method has been used to develop a systematics for delineating regions of continuous transformation involving clustering and ordering associated with a binary phase diagram in which a disordered and an ordered phase are related by a first-order transition under equilibrium conditions. The spinodal decomposition of a supersaturated solid solution producing an ordered phase is generally expected to be preceded by atomic ordering. This ordering process may be heterogeneous or homogeneous depending on the temperature and composition. The different regions of transformation can be mapped into the phase diagram using *loci* of thermodynamic stability with respect to ordering and/or clustering. These ideas have been shown to be relevant for understanding the complex behavior of important binary alloy systems such as Ni–Al, Ni–Ti and Al–Li.

REFERENCES

1. S. Allen and J. W. Cahn, *Acta metall.* **24,** 425 (1976).
2. A. Datta and W. A. Soffa, *Acta metall.* **24,** 987 (1976).
3. D. E. Laughlin, *Acta metall.* **24,** 53 (1976).
4. H. Ino, *Acta metall.* **26,** 827 (1978).
5. W. A. Soffa and D. E. Laughlin, in *Proc. Int. Conf. on Solid → Solid Phase Transformations* (edited by H. I. Aaronson, D. E. Laughlin, R. F. Sekerka and C. M. Wayman), Warrendale, Pa, p. 159 (1982).
6. W. O. Gentry and M. E. Fine, *Acta metall.* **20,** 181 (1972).
7. C. L. Corey, B. Z. Rosenblum and G. M. Greene, *Acta metall.* **21,** 837 (1973).
8. K. Saito and R. Watanabe, *Japan J. Appl. Phys.* **8,** 14 (1969).
9. R. Sinclair, J. A. Leake and B. Ralph, *Physica status solidi* **264,** 285 (1974).
10. U. D. Kulkarni, S. Banerjee and R. Krishnan, *Mater. Sci. Forum* **3,** 111 (1985).
11. A. G. Khachaturyan, T. F. Lindsey and J. W. Morris, *Metall. Trans.* **19A,** 249 (1988).

12. A. G. Khachaturyan, *Progr. Mater. Sci.* **22,** 1 (1978).
13. A. G. Khachaturyan, *Theory of Structural Transformations in Solids.* Wiley, New York (1983).
14. D. deFontaine, *Acta metall.* **23,** 553 (1975).
15. R. O. Williams, *Metall. Trans.* **11A,** 247 (1980).
16. J. W. Cahn and F. Larche, *Acta metall.* **32,** 1915 (1984).
17. W. C. Johnson and C. S. Chiang, *J. appl. Phys.* **64,** 1155 (1988).
18. M. J. Richards and J. W. Cahn, *Acta metall.* **19,** 1263 (1971).
19. T. B. Massalski, in *Phase Transformations*, p. 433. Am. Soc. Metals, Metals Park, Ohio (1970).
20. H. I. Aaronson and K. R. Kinsman, *Acta metall.* **25,** 367 (1977).
21. A. J. Ardell and R. B. Nicholson, *Acta metall.* **14,** 1295 (1967).
22. H. Wendt and P. Haasen, *Acta metall.* **31,** 1649 (1983).
23. S. A. Hill, Ph.D. thesis, Univ. of Cambridge (1980).
24. S. A. Hill and B. Ralph, *Acta metall.* **30,** 2219 (1982).
25. R. E. Beddue, P. Haasen and G. Kostorz, in *Decomposition of Alloys: The Early Stages* (edited by P. Haasen, V. Gerold, R. Wagner and M. F. Ashby). Pergamon Press, Oxford, p. 110 (1984).
26. D. H. Ben Israel and M. E. Fine, *Acta metall.* **11,** 1051 (1963).
27. H. Yoshida, M. Arita, A. Cerri and G. Kostorz, *Acta metall.* **34,** 1401 (1986).
28. G. Kostorz, in *Dynamics of Ordering Processes in Condensed Matter.* Plenum Press, New York.
29. R. Grune and P. Haasen, *J. Physique* **47,** C2 (1986).
30. Frank W. Gayle and John B Vander Sande, *Bull. Alloy Phase Diagr.* **5,** 19 (1984).
31. C. Sigli and J. M. Sanchez, *Acta metall.* **34,** 1021 (1986).
32. R. Nozato and G. Nakai, *Trans. Japan Inst. Metals* **18,** 679 (1977).
33. T. Takahashi and T. Sato, *J. Japan. Inst. Light Metals* **36,** 207 (1986).
34. T. Sato, N. Tanaka and T. Takahashi, *Trans. Japan. Inst. Metals* **29,** 17 (1988).
35. D. E. Laughlin and W. A. Soffa, in *Physical Properties and Thermodynamic Behavior of Minerals*, NATO ASI Series C, Vol. 225, p. 213 (1988).